

Article

Geophysical Surveys to Highlight Buried Ancient Walls of Ugento (Lecce, Italy)

Dora Francesca Barbolla ^{*}, Iaria Miccoli, Immacolata Ditaranto, Giuseppe Scardozzi, Francesco Giuri ,
Ivan Ferrari  and Giovanni Leucci

National Research Council, Institute of Heritage Science, 73100 Lecce, Italy; ilaria.miccoli@cnr.it (I.M.); immacolata.ditaranto@cnr.it (I.D.); giuseppe.scardozzi@cnr.it (G.S.); francesco.giuri@cnr.it (F.G.); ivan.ferrari@cnr.it (I.F.); giovanni.leucci@cnr.it (G.L.)

* Correspondence: dorafrancesca.barbolla@cnr.it

Abstract: Geophysics is a fundamental tool to detect buried structures of archaeological interest through non-destructive techniques. The Messapian city walls in Ugento (Puglia, southern Italy) are of great archaeological importance, and some sections are still visible. In order to locate a stretch of the city walls, geophysical prospections were performed using the low-frequency electromagnetic method and ground-penetrating radar. The surveys were carried out in a peripheral area of Ugento, near a visible section of the city walls. The analysis and interpretation of the measured data revealed clear anomalies that could be ascribed to the city walls that aligned with an adjacent section of the visible walls. Archaeological excavation campaigns found a part of the walls and some important elements, as identified by the geophysical data interpretation.

Keywords: archaeogeophysics; ground-penetrating radar (GPR); electromagnetometer; geophysical prospection; Messapian walls; Ugento



Citation: Barbolla, D.F.; Miccoli, I.; Ditaranto, I.; Scardozzi, G.; Giuri, F.; Ferrari, I.; Leucci, G. Geophysical Surveys to Highlight Buried Ancient Walls of Ugento (Lecce, Italy). *NDT* **2024**, *2*, 204–213. <https://doi.org/10.3390/ndt2030012>

Academic Editor: Fabio Tosti

Received: 20 May 2024

Revised: 9 June 2024

Accepted: 10 June 2024

Published: 22 June 2024



Copyright: © 2024 by the authors. Licensee MDPI, Basel, Switzerland. This article is an open access article distributed under the terms and conditions of the Creative Commons Attribution (CC BY) license (<https://creativecommons.org/licenses/by/4.0/>).

1. Introduction

Archaeogeophysics is a fundamental discipline for exploring and documenting cultural heritage. Geophysical methods are inherently non-destructive, and this feature makes them an essential support tool for archaeologists to provide detailed geometric reconstructions of the buried structures, especially when there is no possibility of direct investigation, and to identify the areas of greater archaeological interest [1]. In this work, we present the results of geophysical surveys performed at Ugento (Lecce, Italy) to locate the ancient walls (Figure 1a).

The ancient walls of Ugento date back to the period of maximum extension of the ancient city center, around the middle of the 4th century B.C. [2]. It was built in a historical moment of great instability and conflict between the Messapians and Tarentines. Subsequently, between the second half of the 4th and 3rd centuries BC, they reinforced and defended the center even during the Second Punic War, when the inhabitants of Uzentum joined Hannibal in the battle against Rome.

The walls enclosed the low hill, on which the modern village of Ugento extends, and part of the flat areas located on its slopes, accounting for a total area of 145 hectares. Today, only a few sectors of the imposing fortifications, 4900 m long in total, are visible. The walls appeared in all their grandeur with a thickness of between 6 and 8 m and originally must have been approximately 6 m high (Figure 1b,c). They consisted of two external curtain walls made of calcarenite blocks, which contained a filling of stones and soil. Along the route of the city walls and near the gates, there were quadrangular towers, which contributed to making it even more powerful.

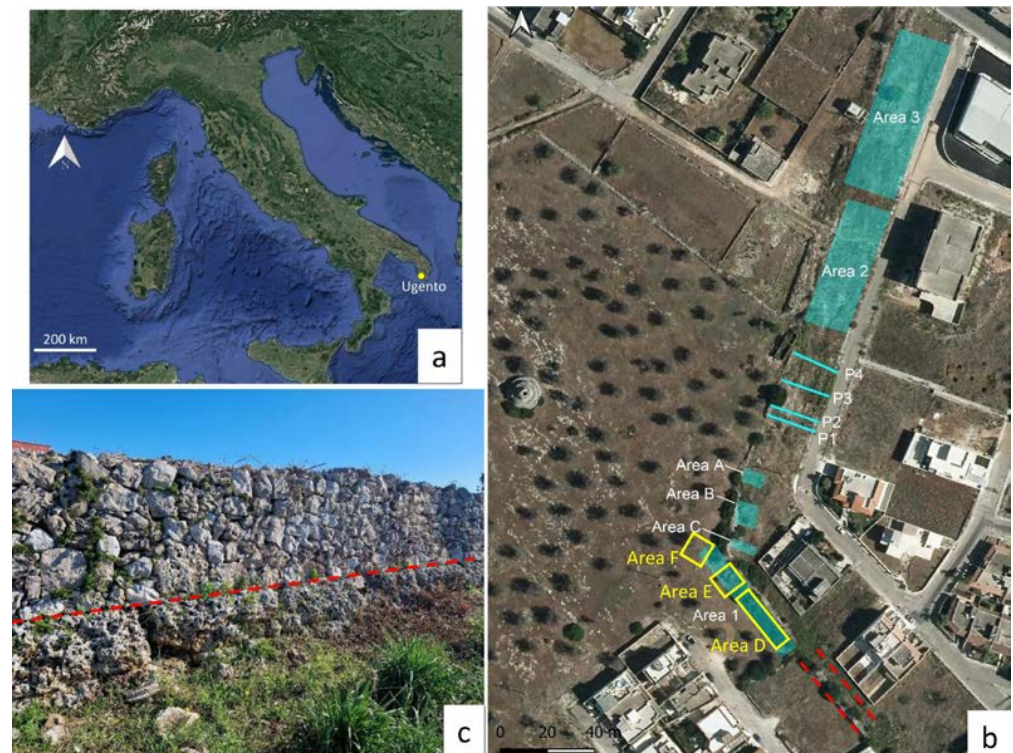


Figure 1. (a) Ugento is located in the southern part of Salento. (b) The studied site is located in a peripheral area of the city: the green areas were investigated with the EM method, while the yellow rectangles-delimited areas were investigated with the GPR method; a section of visible city walls in the adjacent area is highlighted with red dashed lines. (c) The red dashed line highlights the modern dry stone walls over the ancient walls.

Geophysical campaigns carried out previously on Messapian sites [3,4] have shown excellent results in identifying buried structures [3] and reconstructing a stretch of the Messapian city walls and nearby necropolis in the St. Antonio area of Ugento [4].

In the Cupa area, in the immediate western outskirts of the town, a section of the external face of the walls is visible and partially incorporated into the modern drywall (Figure 1b). Here, a section of the internal curtain of the walls, measuring 16 m long, was brought to light in 2006. Such elements guided the hypothesis of the route of the walls. In this study, geophysical surveys were designed according to these archaeological aspects highlighted on the site, with two geophysical campaigns performed employing two methods: the frequency domain electromagnetometry (EM) in the first geophysical campaign and the ground-penetrating radar (GPR) in the second one. Several geophysical methods can be used in archaeological investigations. The GPR has been applied for 25 years in archaeological prospections to map shallow subsurface targets [5]. For logistical reasons, the portion of the surface to be investigated was divided into different areas: 1, 2, and 3 and A, B, and C for the EM method (Figure 2a) and areas D, E, and F for the GPR method (Figure 2b). Their positions and extensions were defined by the conditions of the soil surface under examination and by the expected results compared to the evidence already known, both in trace and following archaeological tests conducted in the past. The soil surface between Area A and Area 2 was uneven due to the presence of shrubs; here, data were acquired along non-equally spaced and non-parallel profiles (P1, P2, P3, and P4).

Some preliminary EM results relating to this work were presented at the MetroArchaeo conference in 2023 [6].

Starting with the results of geophysical prospecting, archaeological excavation campaigns were carried out in an area to find the presence of the structures identified by the geophysical investigations.



Figure 2. Geophysical instruments used for the acquisition of data: (a) electromagnetometer mini-explorer (GF instrument); (b) GPR with multifrequency antenna 200/600 MHz (IDS).

2. Materials and Methods

After a preliminary evaluation of the characteristics and conditions of the areas to be investigated and the extent of the archaeological structures to be identified, we carried out the first geophysical campaign through the application of the electromagnetic method in the frequency domain (FDEM). Electromagnetic prospecting techniques have been used for archaeological purposes since the late 1960s [7,8] and are able to identify a variety of archaeological features [9–12]. This method is mainly used for preliminary surveys of large areas and is one of the fastest geophysical methods. A second geophysical campaign was performed over a smaller area, resulting in high archaeological interest from the EM survey results (Figure 2).

The ability of low-frequency EM instruments to identify archaeological structures is determined by physical issues such as sensor height, coil geometry, and the physical properties of the soil [13]. In this work, we used the CMD mini-explorer probe, a multi-depth electromagnetic conductivity meter by GF Instruments (Figure 2a). It consists of three sensors that allow information to be obtained in three depth ranges. Assuming an increasing distance between the transmitting coil and the receiving coil, the instrument can explore greater depths. The transmitting coil generates a time-varying primary magnetic field, which propagates above and below ground, generating alternating currents (eddy currents) within the soil and the buried objects. The eddy currents create a secondary magnetic field proportional to the rate of change of the primary magnetic field and are measured by receiving coils. The received secondary magnetic field consists of an imaginary part (the quadrature component), which is proportional to the ground conductivity, and a real part (the in-phase component), which is influenced by magnetic properties. In this work, we focus on the interpretation of the electrical conductivity distribution.

Setting the probe to HIGH mode allows measurements with a maximum depth range. In fact, the vertical orientation of magnetic dipoles allows the full depth range to be measured. The survey conducted in this setting allowed the exploration of the subsoil up to a depth of about $z = 2$ m from the ground level. The measurement was carried out in continuous mode by setting the measuring period to 0.2 s and maintaining a constant speed of movement that did not exceed 9 km/h. The out-of-phase and in-phase components were measured as average values obtained during one measuring period.

The acquired data were processed and interpreted to define the subsurface electromagnetic properties. Specifically, subsurface EM energy is influenced by electrical conductivity, dielectric permittivity, and magnetic susceptibility. Electrical conductivity and magnetic susceptibility govern the magnitude of the received EM signal and are therefore used to understand the electrical properties of subsurface materials [1].

Data were acquired in grids with parallel profiles. The spacing between the profiles (Δx) was defined differently for every area: $\Delta x = 2$ m in Areas A, B, and C; $\Delta x = 3$ m in Area 1; and $\Delta x = 5$ m in Areas 2 and 3. These choices were made due to the state of the soil surface.

The acquired data were exported to Res2DInv (v. 4.08) and Res3DInv (v. 3.14) [14]. Considering the quadrature component, after removing the negative values of conductivity, the inversion routine was applied. We obtained the distribution of the electrical resistivity values at several depth ranges.

Ground-penetrating radar is one of the most utilized tools for archaeological prospection due to its high-resolution data and 3D visualization capabilities [15–17]. It allows the collection of a large amount of information on large areas in the first few meters of the subsoil, which is related to the presence of buried bodies or structures of archaeological interest. GPR generates high-frequency impulsive waves (typically between 10 MHz and a few GHz), which are transmitted underground using a suitable transmitting antenna placed in contact with the ground surface. The electromagnetic signal propagates in the medium and is reflected when it encounters a medium with different electromagnetic parameters (discontinuity). The reflected wave that returns to the surface is recorded by a receiving antenna. The control unit amplifies the captured reflection and records it in digital format. By measuring the time interval taken by the pulse to arrive at the buried discontinuity, reflect, and return to the receiver, the position of the reflecting structure can be traced if the propagation velocity is known [1]. The physical parameters that influence the propagation of electromagnetic waves are the electrical conductivity σ (S/m), the dielectric permittivity ϵ , and the magnetic permeability μ . The GPR method obtains good results when operating on resistive soils, allowing the identification of structures with different electromagnetic characteristics compared to the surrounding environment. In the presence of soils with high conductivity, the electromagnetic wave energy is absorbed by the material, causing a drastic signal attenuation and limiting the depth of investigation (i.e., layers of clay or humidity in the subsoil).

In this work, GPR measurements were performed with an IDS Ris Hi-mode system equipped with a dual-band antenna at a nominal central frequency of 200–600 MHz (Figure 2b). A grid of 1 m parallelly spaced profiles was constructed in the three investigated areas (D, E, and F). The time windows were set at 75 ns (600 MHz antenna) and 150 ns (200 MHz antenna), and the B-scan was discretized using 512 samples. The processing of the GPR data consisted of zero timing, background removal, bandpass filtering, and Kirchoff migration. This processing was carried out through the GPRSlice software Version 7.0 [18]. From the shape of the diffraction hyperbolas, we found an average electromagnetic wave velocity equal to 0.085 m/ns. Afterward, the Hilbert transform was applied to the processed data to obtain horizontal depth–time slices. Each slice was retrieved by averaging the data within a time window $\Delta t = 5$ ns, which corresponds to a soil thickness of about 20 cm.

3. Results

3.1. EM Results

EM results provided the identification of several resistivity anomalies related to the presence of significant buried archaeological structures. Area 1 had dimensions of 57×8 m and was oriented in a NW–SE direction in correspondence with a corner of the Messapian city wall, which is buried and partially obliterated by a modern dry stone wall. In detail, the resistivity depth slices showed high resistivity anomalies (greater than 400 Ohm m) potentially related to the presence of buried structures; the elongated shape of these anomalies probably proves the presence of the buried city walls (named W). The presence of this trend was visible in all the layers obtained through the inversion process (Figure 3), i.e., at shallow depths up to a depth of $z = 2$ m. Other high resistivity anomalies (S) could be related to other structures, probably related to the walls.

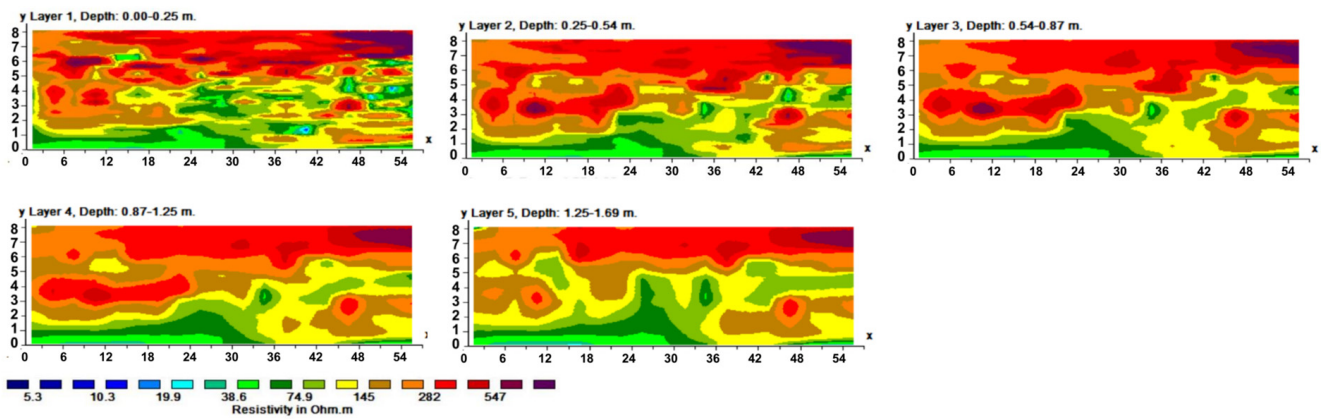


Figure 3. Depth slices relating to Area 1. Layers with different depth ranges: $z = 0\text{--}0.25\text{ m}$; $z = 0.25\text{--}0.54\text{ m}$; $z = 0.54\text{--}0.87\text{ m}$; $z = 0.87\text{--}1.25\text{ m}$; $z = 1.25\text{--}1.69\text{ m}$.

Area 2 ($19 \times 55\text{ m}$) and Area 3 ($23 \times 70\text{ m}$) covered the buried section of the walls, oriented NE–SW. Compared to Area 1, the ground surface of these areas was more uneven and at times covered by shrubby vegetation, although these conditions did not affect the acquisition of geophysical data. Near the corner of the walls to the N of Area 1, three small areas were investigated—Area A ($6 \times 9\text{ m}$), Area B ($10 \times 9\text{ m}$), and Area C ($4 \times 11\text{ m}$)—whose rather limited extension was conditioned by the uneven terrain and the conditions of very invasive vegetation.

In the sector between Area 2 and Area A, which included the NE–SW orientation, data acquisition was performed along independent profiles (P1, P2, P3, and P4), where the passage with the instrumentation was easier. Figure 4 shows the 2D sections on which the high resistivity anomalies detected the presence of walls. The trace of these anomalies is georeferenced as lines (Figure 5, purple lines).

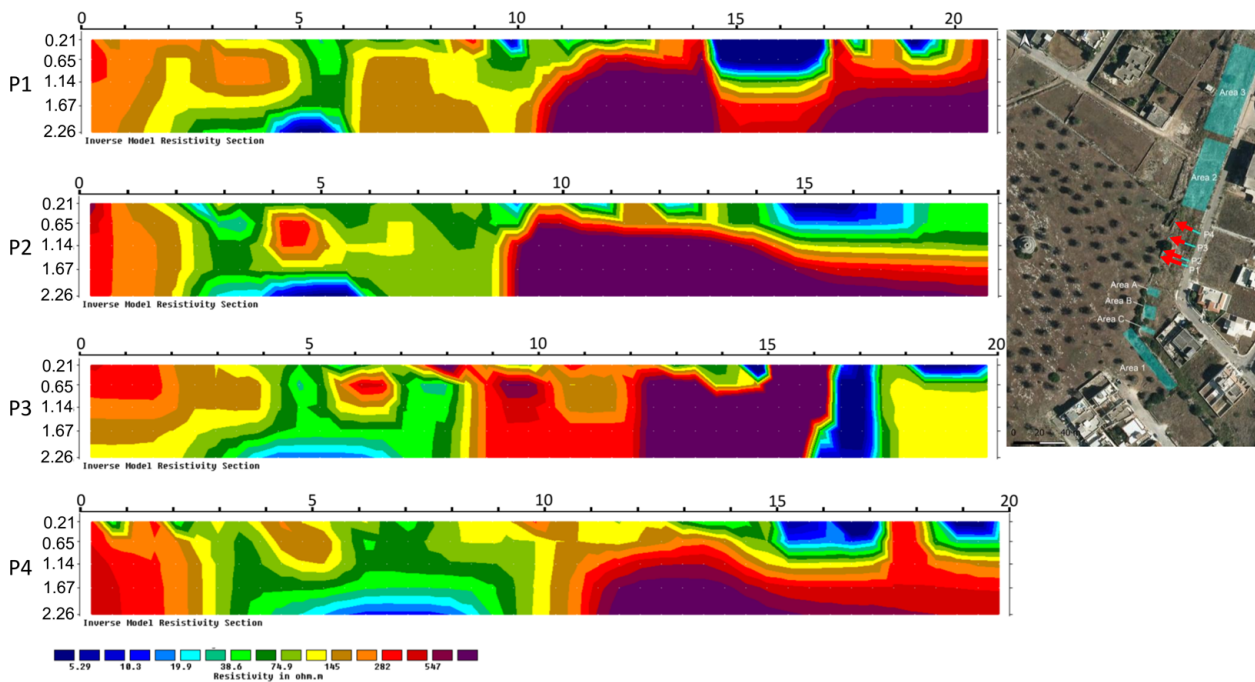


Figure 4. Distribution of the inverse electrical resistivity in profiles P1, P2, P3, and P4. The red arrows in the image on the right show the direction and verse of the acquisition.

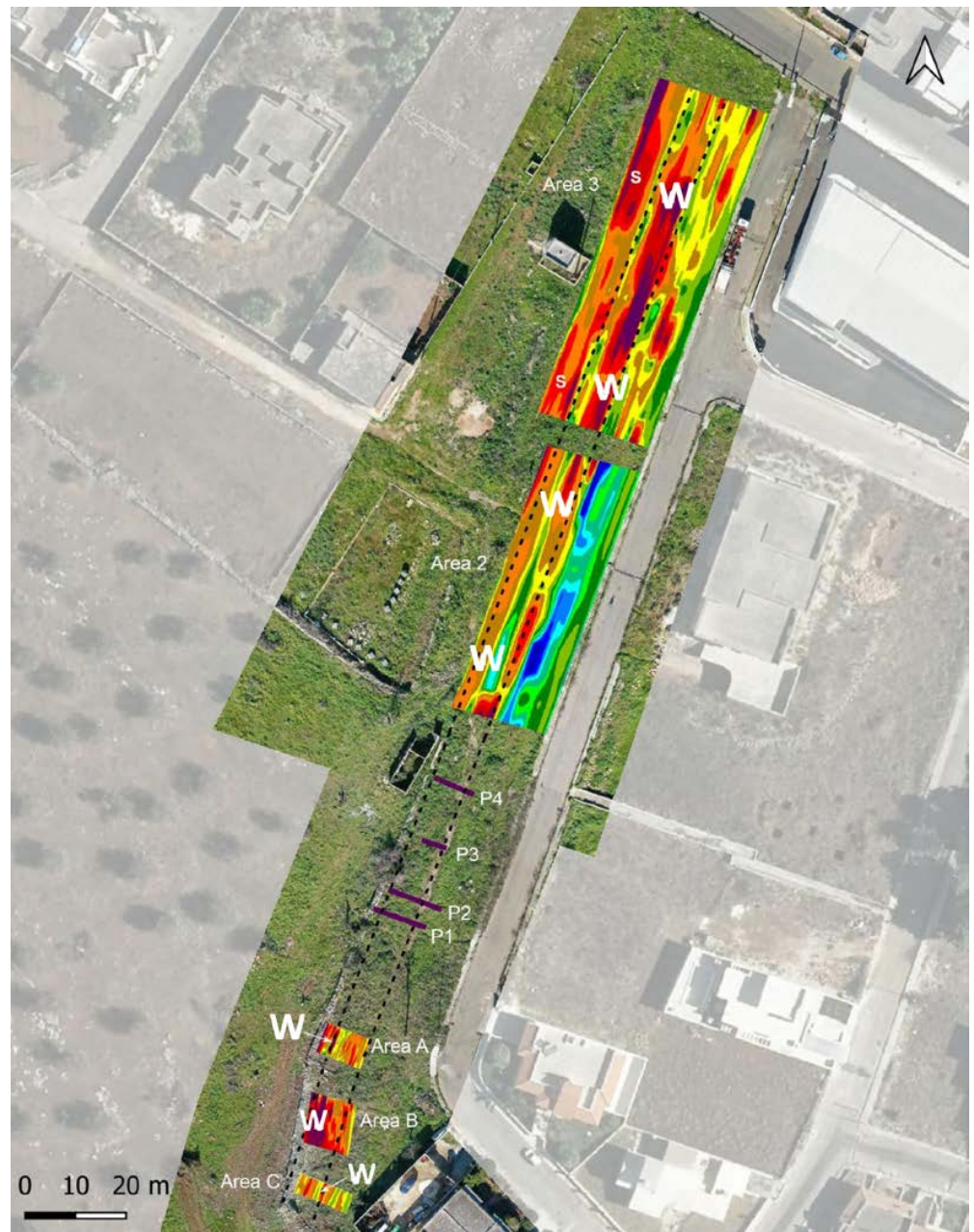


Figure 5. Depth slices relating to the depths of $z = 0.87\text{--}1.25$ m for Area 2 and Area 3 and depths of $z = 0.54\text{--}0.87$ for Area A, Area B, and Area C, georeferenced on drone orthophotos. The high resistivity anomalies (designated by colors from red to purple) named W refer to the buried city wall whose route is indicated by the black dashed line. The width of the anomalies referable to the city walls identified in the individual profiles (P1, P2, P3, and P4) is indicated in purple.

The depth slices relating to depths between $z = 0.87$ and $z = 1.69$ showed linear anomalies with high resistivity along the entire western strip of the area, perfectly aligned with the hypothetical wall layout known from aerial photographic traces. These anomalies correspond to the two external curtains containing the emplèkton attributable to the walls. The average distance between the two bands with high resistivity values was approximately 6.70 m, which is compatible with the known thickness of the walls.

The georeferenced data for Area 1 are shown in Figure 6. As can be seen, the high resistivity anomaly named W runs along the dry stone wall. It is evident that its orientation is aligned with the adjacent section of the visible walls (marked with the dashed black line)

shown in Figure 1b,c. Anomalies named S are probably referable to structures related to the buried walls (named S).



Figure 6. Area 1: georeferenced depth slice (depth of 0.87–1.25 m) over the drone orthophoto, with indication of the anomaly referable to the buried Messapian city walls (named W) and other anomalies probably referable to structures related to the buried walls (named S). The elongated high resistivity anomaly, designated by colors from red to purple (W) and indicated by the black dashed line, aligns with a section of visible city walls (external curtain) in the adjacent area.

3.2. GPR Results

Despite the difficulty in covering the part of the grid very close to the modern wall with the antenna, the GPR measurements also revealed the presence of shallow buried structures (Figure 7), showing anomalies that aligned parallel to the modern drystone walls.

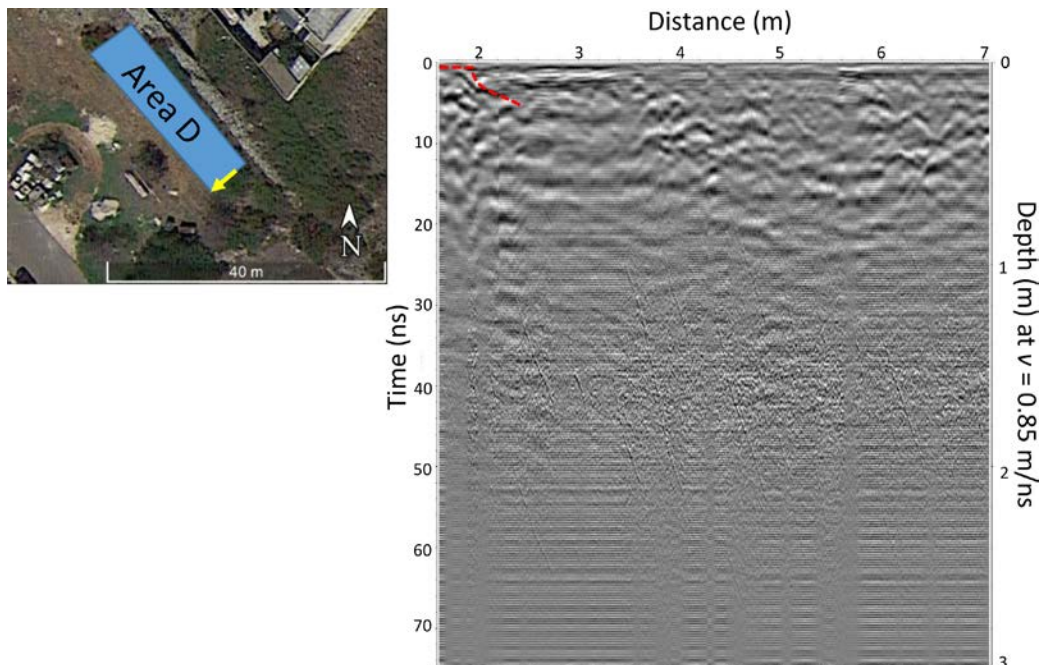


Figure 7. The last profile of Area D starts at a distance of 1.6 m from the start line of the grid due to obstacles on the surface (yellow arrow in the image on the left). The red dashed line highlights a shallow anomaly correlated to the presence of the wall.

Georeferenced time slices showed anomalies that overlapped with the high resistivity anomalies resulting from EM measurements. In particular, in Area F, the trace of the corner of the wall was evident at a depth of 0.6–0.7 m (Figure 8).

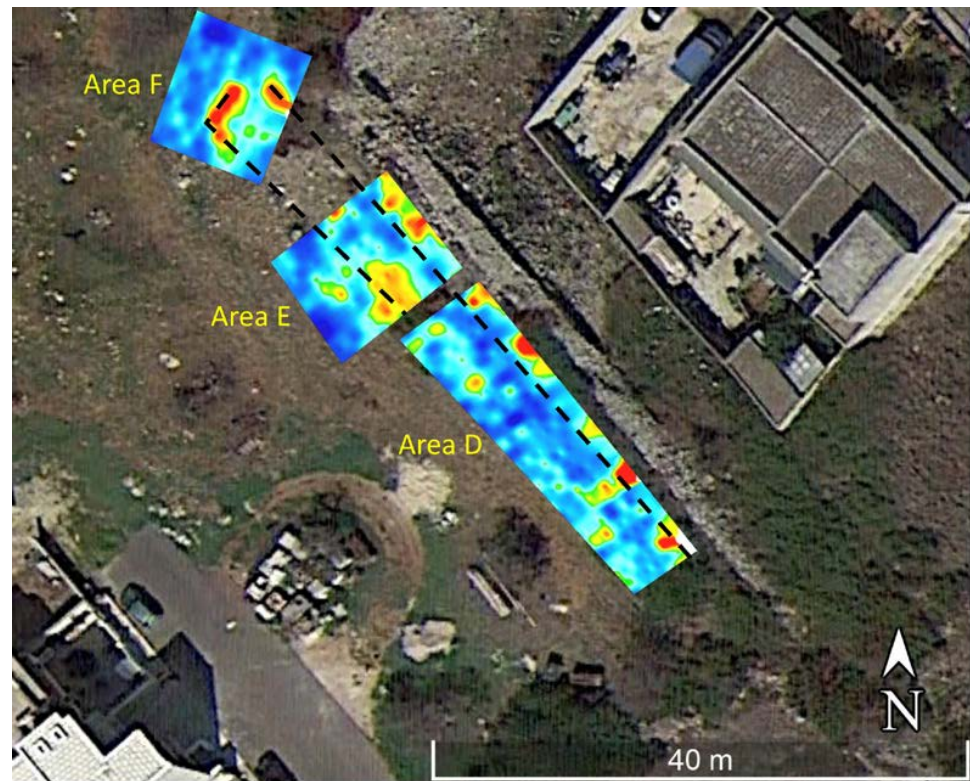


Figure 8. Georeferenced time slices of the GPR survey at depth $z = 0.6\text{--}0.7$ m. Orange to red high-amplitude anomalies are related to buried structures. The black dashed line highlights the alignment of the anomalies found in Area D, Area E, and Area F.

4. Discussion

The results of the geophysical surveys conducted in 2023 in the Cupa area on the immediate western outskirts of the town were used to identify the buried section of the ancient walls of Uzentum, which is the largest ancient center in Messapia. The investigations were also aimed at evaluating the state of conservation of the fortifications and, therefore, planning a targeted excavation campaign.

The archaeological excavations began in January 2024 and confirmed the geophysical results acquired the previous year, documenting a long stretch of the city wall that is preserved for a maximum length of 32 m and a maximum height of 1.60 m (Figure 9a). In this sector, the fortifications are characterized by two curtains with large blocks of calcarenite arranged alternately, head and cutting, with an internal *emplèkton* made up of earth and calcareous stone.

In particular, the internal curtain of the walls is obliterated by a large modern dry stone wall having the same orientation as the ancient walls; the external curtain of the walls (with a thickness of 1.5 m), including the corner, located in the north-western sector of the investigated area, corresponds exactly to the anomalies recorded by the electromagnetic instrumentation at depths reaching up to $z = 1.50$ m. The highlighting of this wall sector provided data about the construction solutions adopted at a particularly vulnerable point of the fortifications. At the corner, an oblique structure 5.5 m long, made with blocks placed head-on, could be attributable to an infill structure made in a second construction phase of the city walls, when probably the timely repair of damage to the walls was necessary (Figure 9b,c). Before the excavation, precisely at this point, electromagnetic investigations had recorded numerous anomalies initially linked to the possible presence

of a tower or other reinforcement structures. The stratigraphic investigations made it possible to understand more clearly the nature of these anomalies, which can actually refer to the blocks placed in secondary positions (Figure 9b,c), because they collapsed or were removed during the demolition phase of the walls in the final decades of the 3rd century B.C. Numerous blocks resulting from the demolition phase of the walls of Ugento were also documented immediately outside the external curtain of the wall.



Figure 9. The excavated area within the investigated areas: Area 1, Area D, Area E, and Area F. (a) orthophoto; (b,c) blocks placed in secondary positions at the corner.

5. Conclusions

The results obtained from the EM and GPR measurements carried out in a peripheral area of Ugento are presented in this paper. The integrated geophysical investigations conducted highlighted the buried ancient city walls, allowing the collection of important new data on the extension of the Messapian city walls. The EM prospecting in particular identified high resistivity anomalies that aligned with the adjacent section of the visible walls. In light of the results, areas of archaeological interest were identified, on which archaeological excavations were carried out and from which sections of the walls were discovered. The present study highlights the importance of geophysical methods as a tool for planning excavation activities and saving time and money.

Author Contributions: Conceptualization, D.F.B. and G.L.; methodology, D.F.B. and G.L.; software, D.F.B. and G.L.; validation, D.F.B., G.L., I.M., I.D., F.G., I.F. and G.S.; formal analysis, D.F.B. and G.L.; investigation, D.F.B., I.M., I.D., F.G., I.F. and G.S.; resources, D.F.B. and G.L.; data curation, D.F.B. and G.L.; writing—original draft preparation, D.F.B.; writing—review and editing, D.F.B., I.M. and G.L.; visualization, D.F.B., G.L., I.M., I.D., F.G., I.F. and G.S.; supervision, G.L., D.F.B. and G.S. All authors have read and agreed to the published version of the manuscript.

Funding: This research received no external funding.

Institutional Review Board Statement: Not applicable.

Informed Consent Statement: Not applicable.

Data Availability Statement: The raw data supporting the conclusions of this article will be made available by the authors on request.

Conflicts of Interest: The authors declare no conflicts of interest.

References

1. Leucci, G. *Nondestructive Testing for Archaeology and Cultural Heritage: A Practical Guide and New Perspective*; Springer: Berlin/Heidelberg, Germany, 2019; ISBN 978-3-030-01898-6.
2. Scardozzi, G. *Topografia Antica e Popolamento Dalla Preistoria Alla Tarda Antichità*; Carta Archeologica di Ugento: Foggia, Italy, 2021.
3. Bianco, C.; De Giorgi, L.; Giannotta, M.T.; Leucci, G.; Meo, F.; Persico, R. The Messapic Site of Muro Leccese: New Results from Integrated Geophysical and Archaeological Surveys. *Remote Sens.* **2019**, *11*, 1478. [[CrossRef](#)]
4. Leucci, G.; De Giorgi, L.; Ditaranto, I.; Miccoli, I.; Scardozzi, G. Ground-penetrating radar and electrical resistivity tomography surveys aimed at the knowledge of the Messapian and Medieval settlement of Ugento (southern Apulia, Italy). *Explor. Geophys.* **2022**, *54*, 33–54. [[CrossRef](#)]
5. Giannino, F.; Leucci, G. *Electromagnetic Methods in Geophysics: Applications in GeoRadar, FDEM, TDEM, and AEM*; Wiley: Hoboken, NJ, USA, 2021; p. 352. ISBN 978-1-119-77098-5.
6. De Giorgi, L.; Barbolla, D.F.; Ferrari, I.; Giuri, F.; Miccoli, I.; Scardozzi, G.; Torre, C.; Leucci, G. Electromagnetic survey to detect a section of the Messapian city walls in Ugento (Lecce). In Proceedings of the MetroArchaeo, Rome, Italy, 19–21 October 2023.
7. Colani, C. *A New Type of Locating Device. I—The Instrument*; Archaeometry: Long Island City, NY, USA, 1966; Volume 9, pp. 3–8.
8. Colani, C.; Aitken, M.J. *A New Type of Locating Device. II—Field Trials*; Archaeometry: Long Island City, NY, USA, 1966; Volume 9, pp. 9–19.
9. Rodrigues, S.I.; Porsani, J.L.; Santos, V.R.N.; DeBlasis, P.A.D.; Giannini, P.C.F. GPR and inductive electromagnetic surveys applied in three coastal sambaqui (shell mounds) archaeological sites in Santa Catarina state, South Brazil. *J. Archaeol. Ical Sci.* **2009**, *36*, 2081–2088. [[CrossRef](#)]
10. Simpson, D.; Lehouck, A.; Verdonck, L.; Vermeersch, H.; Meirvenne, M.V.; Bourgeois, J.; Thoen, E.; Docter, R. Comparison between electromagnetic induction and fluxgate gradiometer measurements on the buried remains of a 17th century castle. *J. Appl. Geophys.* **2009**, *68*, 294–300. [[CrossRef](#)]
11. Simpson, D.; Van Meirvenne, M.; Saey, T.; Vermeersch, H.; Bourgeois, J.; Lehouck, A.; Cockx, L.; Vitharana, U.W. Evaluating the multiple coil configurations of the EM38DD and DUALEM-21S sensors to detect archaeological anomalies. *Archaeol. Prospect.* **2009**, *16*, 91–102. [[CrossRef](#)]
12. Simpson, D.; Van Meirvenne, M.; Lück, E.; Bourgeois, J.; Rühlmann, J. Prospection of two circular Bronze Age ditches with mul-ti-receiver electrical conductivity sensors (North Belgium). *J. Archaeol. Sci.* **2010**, *37*, 2198–2306. [[CrossRef](#)]
13. Bonsall, J.; Fry, R.; Gaffney, C.; Armit, I.; Beck, A.; Gaffney, V. Assessment of the CMD Mini-Explorer, a New Low-frequency Multi-coil Electromagnetic Device, for Archaeological Investigations. *Archaeol. Prospect.* **2013**, *20*, 219–231. [[CrossRef](#)]
14. Loke, M.H. Tutorial: 2-D and 3-D Electrical Imaging Surveys. Geotomo Software. 2024. Available online: <http://www.geotomosoft.com/downloads.php> (accessed on 1 April 2022).
15. Conyers, L.J.; Leckebusch, J. Geophysical Archaeology Research Agendas for the Future: Some Ground-penetrating Radar Examples. *Archaeol. Prospect.* **2010**, *17*, 117–123. [[CrossRef](#)]
16. Conyers, L.B. Innovative Ground-Penetrating Radar Methods for Archaeological Mapping. *Archaeol. Prospect.* **2006**, *13*, 139–141. [[CrossRef](#)]
17. Conyers, L.B. *Ground-Penetrating Radar for Archaeology*, 3rd ed.; Alta Mira Press: Lanham, MD, USA, 2013.
18. Goodman, D. GPR Slice Version 7.0 Manual. 2013. Available online: www.gpr-survey.com (accessed on 1 April 2022).

Disclaimer/Publisher’s Note: The statements, opinions and data contained in all publications are solely those of the individual author(s) and contributor(s) and not of MDPI and/or the editor(s). MDPI and/or the editor(s) disclaim responsibility for any injury to people or property resulting from any ideas, methods, instructions or products referred to in the content.